Study of Pulsed Micro Plasma Arc welding parameters on Weld Bead Geometry of AISI 304L Sheets using Factorial Method

Kondapalli Siva Prasad[1], Chalamalasetti Srinivasa Rao[2], Damera Nageswara Rao[3]

[1] ANITS, Visakhapatnam, India.

[2] Andhra University, Visakhapatnam, India

[3] Centurion University of Technology & Management, Odisha, India.

Correspondence:
Kondapalli Siva Prasad
ANITS, Visakhapatnam, India.
Email: kspanits@gmail.com

Abstract

Pulsed Micro Plasma Arc Welding (MPAW) is a metal joining technique widely used in manufacturing of thin sheet components due to its inherent properties. The present problem is related to fusion butt joint of 0.25 mm thick AISI 304L sheets using the Micro Plasma Arc welding process. The paper discusses the development of mathematical models for weld bead geometry of AISI 304L sheets. Design of experiments based on full factorial design is employed for the development of a mathematical model correlating the important controlled pulsed MPAW process parameters like peak current, back current, pulse rate, and pulse width with front width, back width, front, height, and back height. The developed mode has been checked for adequacy using the Analysis of Varience (ANOVA) technique. Weld bead geometry parameters obtained by the models are found to confirm actual values with high accuracy. Using these models, the effect of pulsed MPAW process parameters on weld bead geometry are studied.

Keywords: Pulsed Current MPAW, AISI 304L, Mathematical Model, Design of Experiments, ANOVA, Weld Bead Geometry

1. Introduction

The plasma welding process was introduced to the welding industry in 1964 as a method of bringing better control to the arc welding process in lower current ranges [1]. Today, plasma retains the original advantages it brought to the industry by providing an advanced level of control and accuracy to produce high quality welds in both miniature and pre-precision applications and to provide long electrode life for high production requirements at all levels of amperage. Plasma welding is equally suited to manual and automatic applications. It is used in a variety of joining operations ranging from welding of miniature components to seam welding to high volume production welding, and many others.

The welding optimization literature frequently reveals correlation among responses. D.K. Zhang et.al. [2] studied the influence of welding current, arc voltage, welding speed, wire feed rate, and magnitude of ion gas flow on front melting width, back melting width, and weld reinforcement of Alternating Current Plasma Arc Welding process of LF6 Aluminum alloy of thickness 3 mm using the Artificial Neural Network-Back Propagation algorithm. Sheng-Chai Chi et al. [3] developed an intelligent decision support system for Plasma Arc Welding of stainless steel plates of thickness range from 3 to 9 mm based on fuzzy Radial Basis Function (RBF) neural network by performing experiments using Taguchi method. Y. F. Hsiao et al. [4] studied the optimal parameters process of plasma arc welding of SS316 of thickness 4 mm by the Taguchi method with Grey relational analysis. Torch stand-off, welding current, welding speed, and plasma gas flow rate (Argon) were chosen as input variables and welding groove root penetration, welding groove width, and front-side undercut were measured as output parameters. K. Siva et al. [5] used central composite rotatable full factorial design matrix and conducted experiments in optimization of weld bead geometry in Plasma arc hardfaced austenitic stainless steel plates using a Genetic Algorithm. A.K. Lakshminarayan et al. [6] predicted the Dilution of Plasma Transferred Arc Hardfacing of Stellite on Carbon Steel using Response Surface Methodology (RSM). V. Balasubramanian et al. [7] used Response Surface Methodology to predict and optimize the percentage of dilution of iron-based hardfaced surface produced by the Plasma transferred arc welding process.

From the earlier works, it has been observed that much work is not reported so far, to investigate the effect of pulsed current MPAW process parameters on stainless steel weld characteristics, and develop related mathematical models to predict the same especially for welding of thin stainless steel sheets. Hence an attempt was made to correlate important pulsed MPAW process parameters to bead geometry of thin AISI 304L stainless steel welds by developing mathematical models. The models developed will be very useful to predict the weld bead geometry parameters for desired bead geometry. A statistically designed experiment based on full factorial design was employed for the development of mathematical models [8].

2. Experimental procedure

Austenitic stainless steel sheets of type AISI 304L 100×50×0.25 mm are welded autogenously with square butt joint without edge preparation. To evaluate the quality of MPAW welds, measurements of the front width, back width, front height, and back height of the weld bead are considered as shown in Fig.1. The chemical composition of AISI 304L stainless steel sheet is given in Table 1. Experiments are conducted using the Pulsed Micro Plasma Arc Welding (MPAW) process. Industrial pure and commercial grade argon gases are used for shielding and back purging, respectively. Automatic voltage control available in the welding equipment is used. Fixture variation effects are not considered as the same setup has been used throughout the experiment. Some of the welding process parameters are fixed based on earlier work and also from the trial run so as to obtain full penetration welds. The fixed pulsed MPAW process parameters and their values are presented in Table 2.

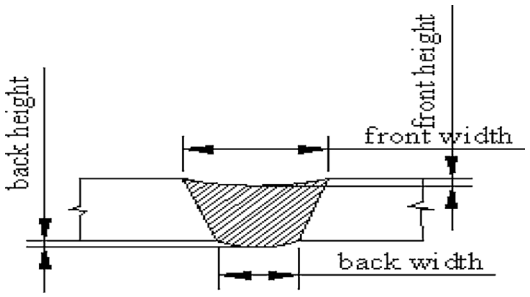

Fig. 1. Typical weld Bead geometry.

Table 1 Chemical composition of austenitic stainless steel (AISI 304L) sheet.

Elements	Chromium	Silicon	Nickel	Carbon	Manganese	Iron
% by weight	18.2%	0.5%	8.5%	0.015%	1.6%	Balance

Table 2 Fixed pulsed MPAW process parameters and their values.

Power source	Secheron Micro Plasma Arc Machine (Model: PLASMAFIX 50E)
Polarity	DCEN
Mode of operation	Pulse mode
Electrode	2% thoriated tungsten electrode
Electrode Diameter	1mm
Plasma gas	Argon & Hydrogen
Plasma gas flow rate	6 Lpm
Shielding gas	Argon
Shielding gas flow rate	0.4 Lpm
Purging gas	Argon
Purging gas flow rate	0.4 Lpm
Copper Nozzle diameter	1mm
Nozzle to plate distance	1mm
Welding speed	260 mm/min
Torch Position	Vertical
Operation type	Automatic

Trial runs are conducted to find the limits of each controllable process parameter so as to obtain full penetration welds, free from any visible defects. Because of computational ease and enhanced interpretability of the models, parameters are converted to coded form for developing mathematical models [9]. The upper limit of a factor is coded as +1 and the lower limit as –1. The levels determined for process variables with their levels, units, and notations for the pulsed MPAW process are given in Table 3.

Table 3 Input variables and their levels.

			Levels	
SI No	**Input Factor**	**Units**	**-1**	**+1**
1	Peak Current	Amperes	6.5	7.5
2	Back Current	Amperes	3.5	4.5
3	Pulse rate	Pulses/second	30	50
4	Pulse width	%	40	60

From the Design of Experiments and due to a wide range of input process parameters, the present work is limited to four factors, two levels, and a full factorial design matrix in order to simplify the present problem. Table-4 shows the 16 sets of coded conditions used in the form of design matrix. The 16 experiments have been formulated as per 24 (two levels and four factors) factorial design. The experimental setup is shown in Fig. 2.

3. Recording the Responses

The samples are cut from the welded specimens and weld Bead geometries are measured using a Metallurgical Microscope (Dewinter Technologie, Model No. DMI-CROWN-II). Photomacrographs of a typical weld specimen showing the bead profile at 100X magnification is presented in Fig. 3.

4. Development of Mathematical Models

A low-order polynomial is employed for developing the mathematical model for predicting weld Bead geometry. If the response is well modeled by a linear function of the independent variables, then the approximating function is the first order model as shown in Equation 1.

Table 4 Welding parameters and responses for the full factorial design.

Exp No	Peak Current (PC)	Back Current (BC)	Pulse rate (P)	Pulse Width (PW)	Front Width	Back Width	Front Height	Back Height
	Amperes	Amperes	Pulses/ second	%	Microns	Microns	Microns	Microns
1	7.5	3.5	30	60	1579.22	1499.50	63.209	57.775
2	6.5	4.5	30	60	1486.59	1361.64	59.137	49.443
3	7.5	4.5	50	60	1383.04	1301.22	53.953	48.422
4	6.5	3.5	50	40	1539.88	1480.60	54.191	49.442
5	7.5	4.5	30	60	1582.92	1506.41	76.886	71.209
6	7.5	3.5	50	40	1404.63	1283.25	71.247	65.947
7	6.5	3.5	30	60	1477.09	1393.14	60.583	54.737
8	6.5	3.5	50	60	1451.98	1372.69	61.896	54.251
9	6.5	3.5	30	40	1530.30	1453.96	57.514	52.538
10	6.5	4.5	50	60	1382.42	1305.11	63.619	58.265
11	7.5	3.5	50	60	1392.70	1337.14	59.083	54.855
12	6.5	4.5	30	40	1543.53	1466.85	42.855	36.559
13	7.5	3.5	30	40	1581.70	1537.70	48.824	42.514
14	7.5	4.5	50	40	1503.05	1436.88	64.101	59.595
15	7.5	4.5	30	40	1547.92	1474.37	52.275	46.553
16	6.5	4.5	50	40	1486.94	1408.72	65.613	58.092

Fig. 2. Experimental setup.

Front Width Back Width Front&Back height

Fig. 3. Photomacrographs of a typical weld specimen.

$$Y = \beta + \beta_1 x_1 + \beta_2 x_2 + \ldots\_\beta_x X_x + \in \quad (1)$$

The regression coefficients were calculated using MINITAB14 software and developed models with welding parameters in coded form are shown in Equations 2, 3, 4, 5.

Front Width =1492.12+(38.45*X1)-(6.42*X2)+(7.07*X3)+(5.85*X4) +(26.12*X1*X2)+(9.6*X1*X3)
+(24.67*X1*X4)+(2.1*X2*X3)
+(4.17*X2*X4)-(7.86*X3*X4)
+(16.27*X1*X2*X3)+
(28.66*X1*X2*X4)-(10.35*X1*X3*X4)
-(15.91*X2*X3*X4) (2)

Back Width =1413.7+(46.21*X1)-(5.53*X2)-(1.79*X3)+(8.53*X4)-(34.34*X1*X2)+(15.69*X2*X3)+
(27.73*X1*X4)+(9.46*X2*X3)-(1.52*X2*X4)-(9.7*X3*X4)
+(10.7*X1*X2*X3)+(28.4*X1*X2*X4)-(10.32*X1*X3*X4)-(12.8*X2*X3*X4) (3)

Front Height = 59.687-(1.253*X1)-(0.756*X2)+(3.032*X3)-(4.457*X4)
+(1.146*X1*X2)+(3.509*X1*X3)
-(1.707*X1*X4)-(1.891*X2*X3)
+(0.676*X2*X4)-(0.639*X3*X4)
+(0.937*X1*X2*X3)-(0.304*X1*X2*X4)+(0.529*X1*X3*X4)+ (2.929*X2*X3*X4)

(4)

Back Height = 53.761-(1.212*X1)-(0.513*X2)+(2.845*X3)-(4.545*X4)
+(0.637*X1*X2)+(3.731*X1*X3)
-(1.436*X1*X4)-(1.886*X2*X3)+
(0.671*X2*X4)-(0.795*X3*X4)+
(0.571*X1*X2*X3)-(0.195*X1*X2*X4)+(1.25*X1*X3*X4)
+(3.562*X2*X3*X4) (5)

where X1, X2, X3, X4 are coded values of welding parameters namely peak current, back current, pulse rate, and pulse width.

5. Checking the adequacy of the mathematical models

The adequacy of the developed models is tested using the ANOVA technique. As per this technique, if the calculated value of Fratio of the developed model is less than the standard Fratio (from F-table) value at a desired level of confidence (say 99%), then the model is said to be adequate with in the confidence limit. ANOVA test results of all the responses are presented in Table 5. The ANOVA table (Table 5) reveals that all the calculated F values are less than standard table F value 8.68; hence the developed mathematical models are adequate.

Table 5 ANOVA test results.

ANOVA for Front Width					
Source	DF	Seq SS	Adj SS	Adj MS	F
Main Effects	4	25659	25659	6415	1.40
2-Way Interactions	6	23462	23462	3910	0.85
3-Way Interactions	4	23142	23142	5785	1.26
Residual Error	1	4575	4575	4575	
Total	15	76837			
R-Sq = 94.05%					
ANOVA for Back Width					
Source	DF	Seq SS	Adj SS	Adj MS	F
Main Effects	4	35868	35868	8967	2.47
2-Way Interactions	6	38078	38078	6346	1.75
3-Way Interactions	4	19057	9057	4764	1.31
Residual Error	1	3633	3633	3633	
Total	15	96636			
R-Sq = 96.24%					

ANOVA for Front Height					
Source	DF	Seq SS	Adj SS	Adj MS	F
Main Effects	4	499.22	499.22	124.80	2.48
2-Way Interactions	6	335.64	335.64	55.94	1.11
3-Way Interactions	4	157.23	157.23	39.31	0.78
Residual Error	1	50.23	50.23	50.23	
Total	15	1042.32			
R-Sq = 95.18%					
ANOVA for Back Height					
Source	DF	Seq SS	Adj SS	Adj MS	F
Main Effects	4	487.77	487.77	121.94	4.31
2-Way Interactions	6	336.44	336.44	56.07	1.98
3-Way Interactions	4	233.81	233.81	58.45	2.06
Residual Error	1	28.32	28.32	28.32	
Total	15	1086.34			
R-Sq = 97.39%					

Where SS =Sum of Squares, MS=Mean Square, F=Fishers ratio

6. Results & Discussion

From the developed mathematical models, predicted values of weld bead geometry are calculated and presented in Table 6.

Table 6 Welding parameters and responses for the full factorial design.

	Front Width (Microns)		Back Width (Microns)		Front Height (Microns)		Back Height (Microns)	
Run Order	Actual	Predicted	Actual	Predicted	Actual	Predicted	Actual	Predicted
1	1579.22	1562.31	1499.5	1484.43	63.209	61.4371	57.775	56.4446
2	1486.59	1469.68	1361.64	1346.57	59.137	57.3651	49.443	48.1126
3	1383.04	1399.94	1301.22	1316.28	53.953	55.7249	48.4222	49.7524
4	1539.88	1556.79	1480.6	1495.67	54.191	55.9629	49.422	50.7524
5	1582.92	1566.01	1506.41	1491.34	76.886	75.1141	71.209	69.8786
6	1404.63	1421.54	1283.25	1298.32	71.247	73.0189	65.947	67.2774
7	1477.09	1460.18	1393.14	1378.07	60.583	58.8111	54.737	53.4066
8	1451.98	1435.07	1372.69	1357.62	61.896	60.1241	54.251	52.9206
9	1530.3	1513.39	1453.96	1438.89	57.514	55.7421	52.538	51.2076
10	1382.42	1365.51	1305.11	1290.04	63.619	61.8471	58.265	56.9346
11	1392.7	1409.60	1337.14	1352.21	59.083	60.8546	54.855	56.1854
12	1543.53	1560.44	1466.85	1481.92	42.855	44.6269	36.559	37.8864
13	1581.7	1564.79	1537.7	1522.63	48.824	47.0521	42.514	41.1836
14	1503.05	1519.95	1436.88	1451.95	64.101	65.8729	59.595	60.9254
15	1547.92	1564.83	1474.37	1489.44	52.275	54.0469	46.553	47.8834
16	1486.94	1503.85	1408.72	1423.79	65.613	67.3849	58.092	59.4224

The individual effect of different pulsed MPAW process parameters on the weld Bead geometry were analyzed and are presented graphically in Fig. 4, 5, 6, 7 for quick analysis.

From Fig. 4, 5, 6 & 7 it is understood that the peak current & pulse had more significant effect on weld bead geometry compared to back current and pulse width.

As the peak current and pulse rate increases, heat input also increases, which leads to higher penetration and hence wider front and back widths. As the widths become wider the slopes become smaller, thereby decreasing the front and back heights. As the pulse rate increases the weld bead geometry parameters decreases because of lower cooling rate of weld metal. Back current is helpful in maintain the continuous arc, however increasing the back current decrease the weld bead geometry parameters because of large variation in pulse rate.

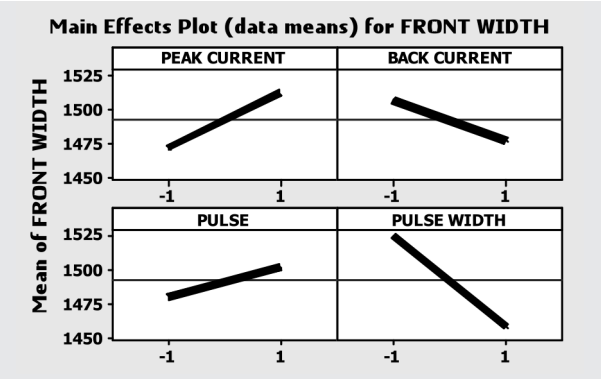

Fig. 4. Main effects for Front Width.

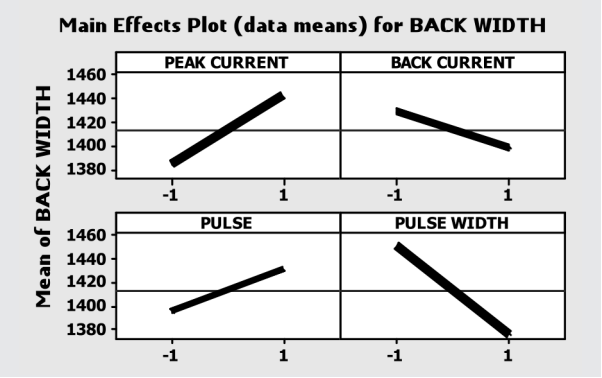

Fig. 5. Main effects for Back Width.

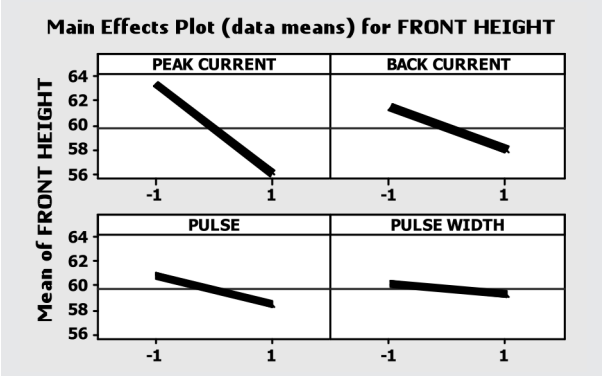

Fig. 6. Main effects for Front Height.

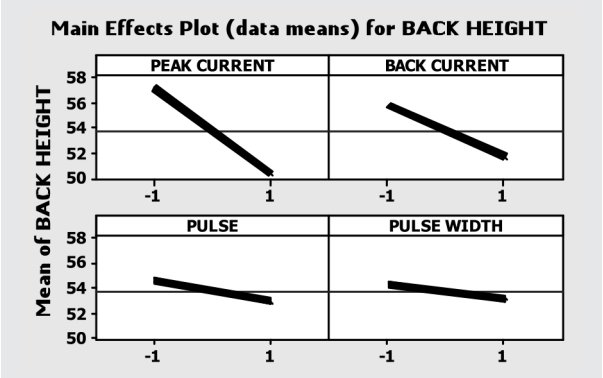

Fig. 7. Main effects for Back Height.

The contribution of each process parameter on weld bead geometry parameters are presented in Figs. 8, 9, 10, 11. It is understood that for front width and back width, peak current and pulse rate have a positive effect, whereas back current and pulse width have a negative effect. For front height, and back height all the welding parameters have a negative effect.

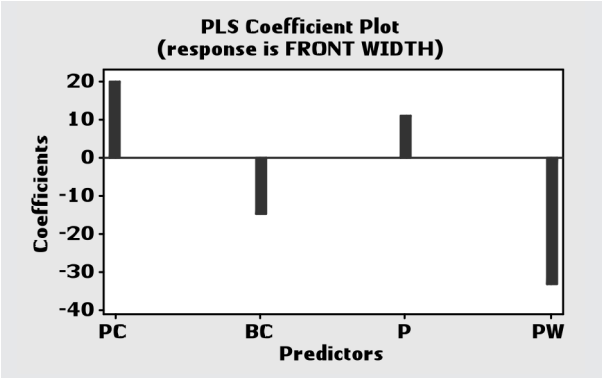

Fig. 8. Contribution plot for Front Width.

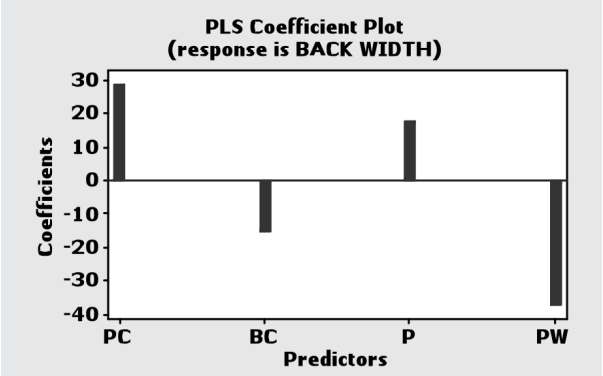

Fig. 9. Contribution plot for Back Width.

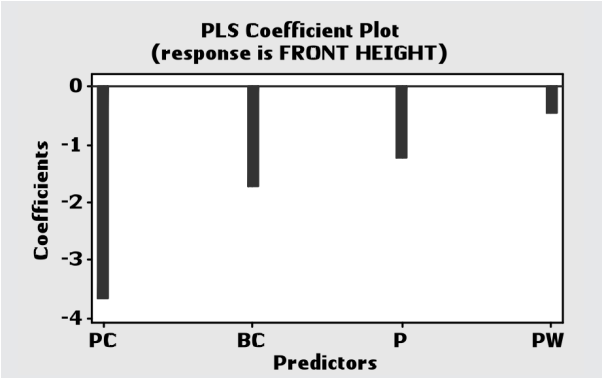

Fig. 10. Contribution plot for Front Height.

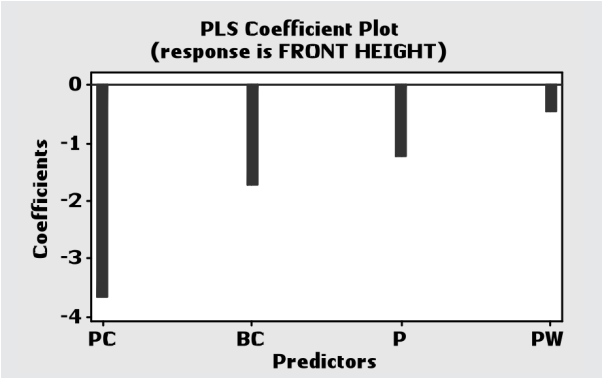

Fig. 11. Contribution plot for Back Height.

7. Conclusion

The present work establishes the following conclusions:

- From the developed mathematical models, predicted values of weld bead geometry parameters were computed and found to be very close to actual values.
- Front Width & Back Width increase with Peak Current & Pulse, whereas they decrease with Back Current and Pulse Width.
- Front Height and Back Height decrease with Peak Current, Back Current, Pulse, and Pulse Width.
- Peak Current and Pulse have a positive effect on Front Width & Back Width, whereas Back Current and Pulse Width have a negative effect.
- All the process parameters have negative effect on Front Height and Back Height.
- The present study is limited to four process parameters namely, peak current, back current, pulse, and pulse width for predicting the weld bead geometry. One may consider other factors like welding speed, distance of nozzle stand, plasma and shielding gas flow rates, and more levels for improving the mathematical model.

Acknowledgements

We express our sincere thanks to Shri. R. Gopla Krishnan, Director, M/s Metallic Bellows (I) Pvt Ltd, Chennai for his support to carry out experimentation work.

8. References

[1] Plasma Welding: more accurate, better control at lower currents, Modern Application News, December 1999.

[2] D.K. Zhang and J.T. Niu, Application of Artificial Neural Network modeling to Plasma Arc Welding of Aluminum alloys, Journal of Advanced Metallurgical Sciences, Vol. 13, No. 1, pp. 194 - 200, 2010.

[3] Sheng-Chai Chi, LI-Chang Hsu, A fuzzy Radial Basis Function Neural Network for Predicting Multiple Quality characteristics of Plasma Arc Welding, IEEE, 0-7803-7078-3/01, pp. 2807 - 2812, 2001.

[4] Y.-F. Hsiao, Y.-S. Tarng, and W.-J. Huang, Optimization of Plasma Arc Welding Parameters by Using the Taguchi Method with the Grey Relational Analysis, Journal of Materials and Manufacturing Processes, Vol. 23, pp. 51 - 58, 2008.

[5] K. Siva, N. Muragan, R. Logesh, Optimization of weld bead geometry in Plasma transferred arc hardfacing austenitic stainless steel plates using genetic algorithm, Int. J. Adv. Manuf. Technol., Vol. 41, No. 1 - 2, pp. 24 - 30, 2008.

[6] A.K. Lakshinarayanan, V. Balasub-ramanian, R. Varahamoorthy, and S. Babu-, Predicting the Dilution of Plasma Transferred Arc Hardfacing of Stellite on Carbon Steel using Response Surface Methodology, Metals and Materials International, Vol. 14, No. 6, pp. 779 - 789.

[7] V. Balasubramanian, A.K. Lakshmi-narayanan, R Varahamoorthy, and S. Babu, Application of Response Surface Methodolody to Prediction of Dilution in Plasma Transferred Arc Hardfacing of Stainless Steel on Carbon Steel , Science Direct, Vol. 16, No. 1, pp. 44 - 53, 2009.

[8] Montgomery DC, Design and analysis of experiments, 6th edn. Wiley, New York, 2005.

[9] Giridharan P.K, Murugan N, Effect of pulsed gas tungsten arc welding process parameters on pitting corrosion resistance of type 304L stainless steel welds, Corros. J. , Vol. 63, No. 5, pp. 433 - 441, 2007.